Molecular Beam Epitaxy Grown Group-IV Alloys: Ideal Candidate for Momentum(*k*)-Space Carrier Separation Photodetectors

Tyler T. McCarthy[1*], Zheng Ju[1,2], Stephen Schaefer[1], Xin Qi[1], Allison McMinn[1], Shui-Qing Yu[3], and Yong-Hang Zhang[1]
[1]School of Electrical, Computer, and Energy Engineering, Arizona State University, Tempe, AZ 85287, USA
[2]Department of Physics, Arizona State University, Tempe, AZ 85287, USA
[3]Department of Electrical Engineering, University of Arkansas, Fayetteville, Arkansas 72701, USA
*Corresponding author: ttmccart@asu.edu

Recently, we proposed the momentum(*k*)-space carrier separation (*k*-SCS) concept that combines the advantages of both direct and indirect bandgaps for light detection/conversion devices. The basic principle is to have a direct bandgap in a semiconductor that has a slightly larger bandgap than the indirect fundamental bandgap, giving a thermalization barrier, $\Delta_{\Gamma\text{-L}}$, such as $3k_BT$, for electrons at the conduction band edge. In this example, the Γ-valley minimum is $3k_BT$ higher in energy than the *L*-valley minimum. The sharp absorption edge of the direct bandgap energy, $E_{g,\Gamma}$, appears at just slightly ($3k_BT$) higher in energy than the slow onset of the absorption edge at the indirect bandgap, $E_{g,L}$,. Under light illumination, electrons are excited to the direct *Γ*-valley in the conduction band while leaving holes in the valence band edge at the symmetry point of *Γ*. The large majority of photogenerated electrons in the direct *Γ*-valley will quickly thermalize at a sub-picosecond time scale to the lower energy indirect *L*-valley. These electrons in the *L*-valley will recombine with the holes in the valence band at a time scale of tens of microseconds to milliseconds. Both carriers, electrons and holes, are transported in real space but with different momentums, i.e. separately in *k*-space, to their corresponding contacts with negligible recombination. This clever design not only improves photogenerated carrier lifetime, similar to indirect bandgap semiconductors, but also offers a large absorption coefficient, similar to direct bandgap semiconductors.

Group-IV alloys such as GeSn are a model material system to demonstrate the novel idea as photodetectors with Sn compositions near the indirect-to-direct bandgap transition are predicted to have greater detectivity than conventional IV-VI and III-V compound photodetectors at room temperature, and comparable detectivity to InAs detectors operating at 77 K. GeSn samples with $\Delta_{\Gamma\text{-L}}$ between $0.4k_BT$ and $3k_BT$ were grown by MBE on Ge substrates for MWIR (2 to 5 µm). Substrate surfaces were first cleaned using HF and HCl solution prior to a UHV outgas at 550 ˚C. A Ge buffer was grown at a substrate temperature of 500 ˚C before cooling down to 200 ˚C for GeSn growth. Ge effusion cell was held constant while Sn effusion cell was varied between 825 to 900 ˚C to obtain designed composition. RHEED showed a streaky (2x1) surface reconstruction pattern that transitions to a (1x1) with increasing Sn. Introducing Si expands the wavelength coverage range to 2 ~ 22 µm, making it ideal for MWIR, LWIR and VLWIR applications. More details of the theory and experiments will be reported at the conference.

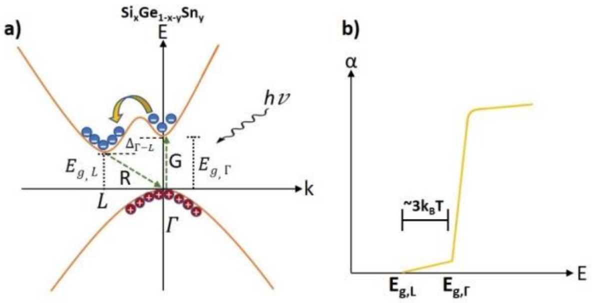

Fig. 1. Schematic illustrating momentum(*k*)-space carrier separation using $Si_xGe_{1-x-y}Sn_y$ as an example material. a) An electron thermalization barrier, $\Delta_{\Gamma\text{-}L}$, on the order of k_BT is introduced between the *Γ*- and *L*-valleys in the conduction band. The barrier height $\Delta_{\Gamma\text{-}L}$ is given by the difference between the indirect bandgap (*L*-*Γ* transition, $E_{g,L}$) and the direct bandgap (*Γ*-*Γ* transition, $E_{g,\Gamma}$). Photogenerated electrons are excited mainly into the *Γ* valley due to higher absorption coefficient of the direct *Γ*- *Γ* transition (G), and then quickly thermally relax to the indirect *L* valley at a lower energy, where recombination (R) takes place at a much lower rate, resulting in a long lifetime. b) The absorption coefficient of the higher energy direct bandgap is much greater than the indirect bandgap which lies several k_BT below.

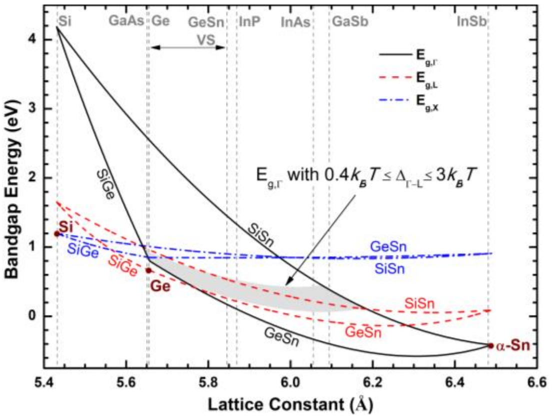

Fig. 2. Calculated bandgap energies (*Γ*-*Γ*, *L*-*Γ*, *X*-*Γ*) of the SiGe, GeSn, and SiSn binaries as a function of their lattice constants at 300 K. The shaded region indicates the SiGeSn alloys with direct bandgaps that satisfy the requirement $0.4k_BT \le \Delta_{\Gamma-L} \le 3k_BT$, a range for the thermalization barrier.

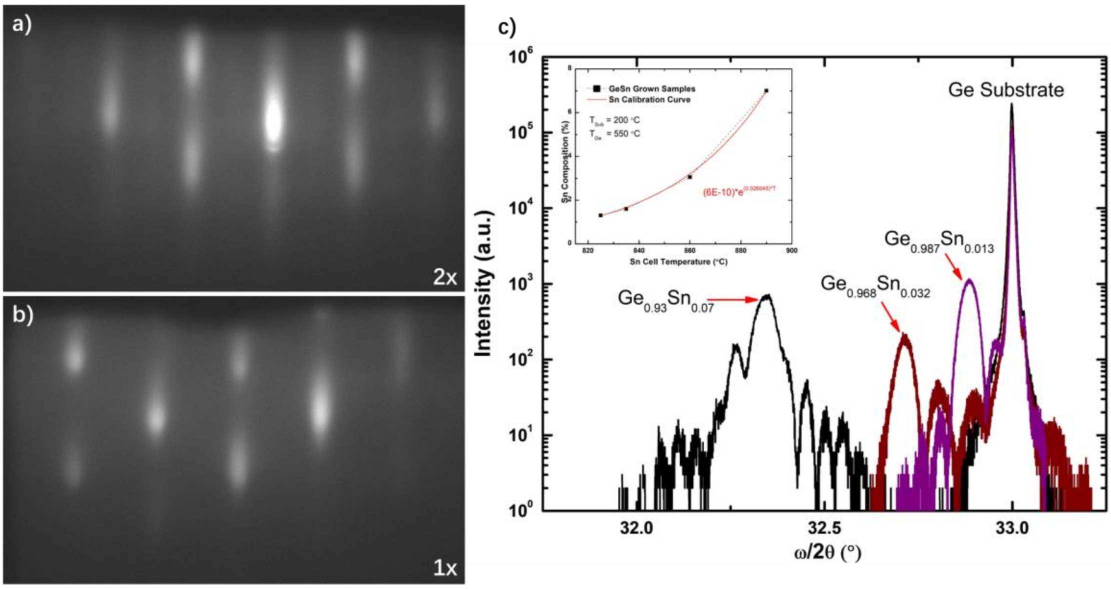

Fig. 3. (a,b) RHEED reconstruction changes from (2x) to (1x) with increasing Sn composition and (c) XRD spectra of GeSn samples towards achieving *k*-SCS. (inset) Sn composition versus Sn cell temperature calibration curve for constant substrate and Ge cell temperatures